

## EXPORT observations of 1998 Microlensing events

Yiannis Tsapras<sup>1</sup>, Rachel A. Street<sup>1</sup>, Keith Horne<sup>1</sup>, Alan Penny<sup>2</sup>, Fraser Clarke<sup>3</sup>, Hans Deeg<sup>4,5</sup>, Francisco Garzon<sup>4</sup>, Simon Kemp<sup>4</sup>, Maria Rosa Zapatero Osorio<sup>4</sup>, Alejandro Oscoz Abad<sup>4</sup>, Santiago Madruga Sanchez<sup>4</sup> and EXPORT<sup>6</sup> team

<sup>1</sup>School of Physics and Astronomy, Univ. of St Andrews, Scotland  
KY16 9SS

<sup>2</sup>Rutherford Appleton Laboratories, Oxon, England

<sup>3</sup>Institute of Astronomy, Cambridge

<sup>4</sup>Instituto de Astrofisica de Canarias

<sup>5</sup>Instituto de Astrofisica de Andalucia, Granada

<sup>6</sup><http://export.ft.uam.es/>

**Abstract.** During the summer of 1998 the EXPORT collaboration monitored microlensing event light-curves using CCD cameras on the IAC 0.8m telescope to evaluate the prospect of hunting for Jupiter-mass planets orbiting stars that are lensing galactic bulge sources. The results obtained are presented here. We argue that daily monitoring of microlensing events in the galactic bulge using small telescopes from Northern sites is a feasible method for detecting Jupiters.

### 1. Introduction

Microlensing (Paczynski 1996) involves the gravitational deflection of light from a background star (source) as a massive stellar object (lens) passes in front of it. This results in two images of the background source on either side of the lens positions. For sources in the galactic bulge, the image separation is of the order of milliarcseconds and thus unresolvable. What is actually observed in microlensing events is a variation of the brightness of the source as the lens moves in front of it.

The range of influence of a point lens is given by its Einstein ring radius

$$R_E = \sqrt{\frac{4GM_L D_L D_{LS}}{c^2 D_S}}. \quad (1)$$

$D_{LS}, D_S, D_L$  are the lens-source, observer-source and observer-lens distances, respectively. The single point lens equation of gravitational lensing has two solutions corresponding to the positions of the images. If the source and the lens are perfectly aligned then the images merge into a ring of radius  $R_E$  around the lens. For all other positions of the source, one image lies inside and the other outside the ring (see figures 1, 2). The total amplification is given by:

$$A = \frac{u^2 + 2}{u(u^2 + 4)^{1/2}}, \quad (2)$$

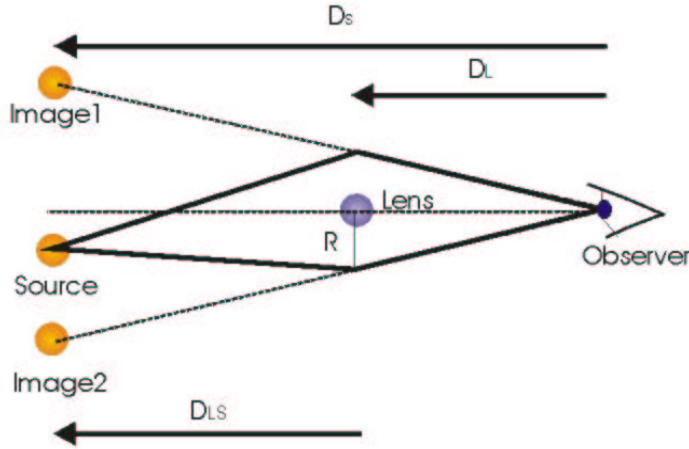


Figure 1. Schematic diagram of Microlensing geometry.  $D_L, D_S, D_{LS}$  are the observer-lens, observer-source and lens-source distances respectively.  $R$  denotes the Einstein ring radius.

where  $u = R_S/R_E$ ,  $R_S$  is the separation on the lens plane between the lens and the source.  $R_E$  is the Einstein ring radius of the lens.

## 2. Microlensing Lightcurves

Sources that lie inside the Einstein ring will have peak magnifications  $A$  in excess of 1.34. The resulting light-curve is axially symmetric and  $A$  increases as the source impact parameter  $u_{min}$  decreases. Galactic bulge lensing events have typical timescales  $t_E=10-100$  days (Bennet & Rhie 1996).

If two or more lensing masses are involved in the lensing event, the magnification pattern is changed so that at certain positions on the sky their individual lensing strengths combine. These positions are called caustics and when the source crosses them the event light-curve becomes distorted. By correctly assessing such light-curve anomalies, the presence (or absence) of planetary companions can be deduced.

## 3. Monitoring microlensing events

To quantify planetary anomalies in a light-curve, events in progress must be imaged very frequently. The planetary effects last for 1-3 days when a Jupiter mass companion is involved (Gould & Loeb 1992). To correctly estimate the duration and structure of the anomalous peak, and thus place restrictions on the planet-to-star mass ratio and the planetary position relative to the lens, we require the fitting of several points. Ideally, a search for Jupiters would employ hourly imaging, which also increases the possibility of detecting deviations caused by Earth-mass planetary companions, whose planetary deviations last for

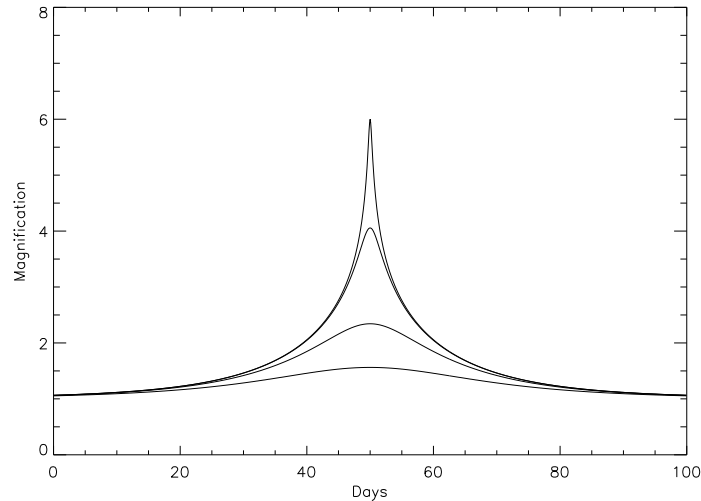


Figure 2. Lightcurves produced by a source star passing behind a lens for four different impact parameters. The impact parameters for the curves from top to bottom are: 0.01, 0.06, 0.3, 0.7

a few hours only. However, daily sampling from a northern site should suffice to detect Jupiters, with one or two data points deviating from the unperturbed light-curve assuming the event was followed closely.

In the summer of 1998 the EXPORT team decided to test this assumption by following up on microlensing events in the galactic bulge. The IAC 0.8m telescope on Tenerife was used for one hour per night for a period of four and a half months (15 May - 30 Sept, see table 1).

Table 1. 1998 IAC Observations

Event	Nights	Filter	Dates
98-BLG-07	3	R	May 31, June 04, 20
98-BLG-18	6	R	May 15, 18, June 03, 08, 12
98-BLG-26	5	R	June 18, 21, 27, 29, Aug 16
98-BLG-35	12	R	July 04, 05, 06, 10, 11, 27, 29, 30, 31 Aug 01, 07, 10
98-BUL-26	4	R	Aug 13, 15, 18, 19
98-BLG-42	15	R	Aug 24, 25, 26, 27, 28, 29, 30, Sept 02, 03, 04, 05, Sept 06, 15, 19, 20
98-BUL-34	7	R	Sept 21, 22, 23, 24, 26, 29, 30

Several ongoing microlensing events were monitored. On each observing night, three 600-sec, R-band images were taken. The CCD size was 1024x1024 pixels, covering a sky area of 7.3x7.3 arcmin and the typical airmass was between 1.5 and 2. The microlensing events were recorded often with accuracies at best  $\sim 1$ -2 % for a star of 16th magnitude and more typically  $\sim 3$ -4 % at 18th

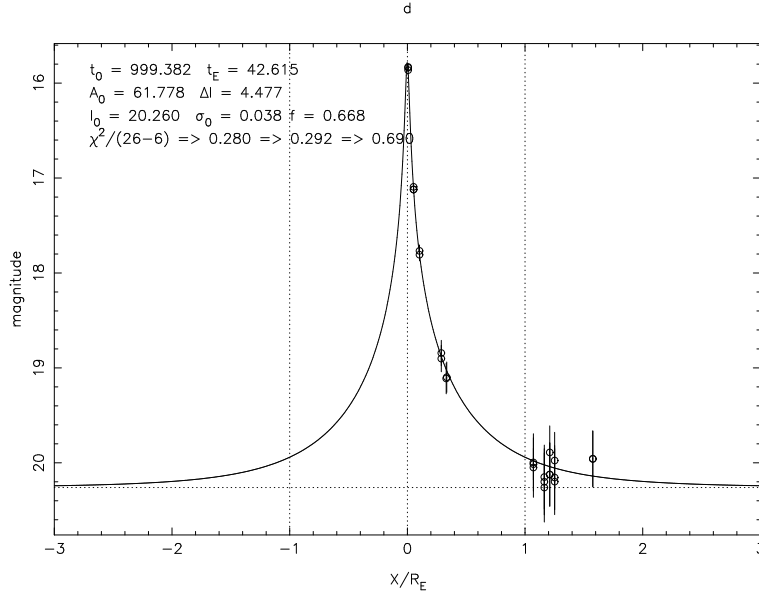


Figure 3. Fitted light-curve for the event 98BLG35. R-magnitude is plotted versus time in units of  $t_E$ . The estimated event parameters are shown on the top left of the plot.

magnitude. No planetary deviations from the event light-curves were found. This was not unexpected since the gaps in temporal sampling were of appreciable size.

#### 4. Crowded field photometry at high airmass

Our crowded field photometry of the CCD data was performed using the STAR-MAN stellar photometry package (A. Penny 1995) in a semi-automated data reduction pipeline. All frames were debiased and flat-fielded in the usual manner and the target was identified from finder charts. Several stars were selected manually on which photometry was to be performed. Apart from the target, these included i) several bright, unsaturated stars that were used for the PSF generation and ii) a selection of “error stars” of constant brightness, comparable to that of the target at each stage of the lensing event, which were used to estimate the RMS uncertainty on the measured target magnitude at each stage of its brightness variation. All images were aligned and crowded field PSF-fitting photometry was performed on the stars on all frames. Stars with poor fits were excluded from further processing. The measured star images were expressed as differential magnitudes relative to a set of 25 reference stars.

The theoretical errors were calculated using the standard formula

$$\sigma^2 = \sigma_0^2 A_{psf} + \frac{f_* t}{G} + \frac{f_s t A_{psf}}{G} \quad (3)$$

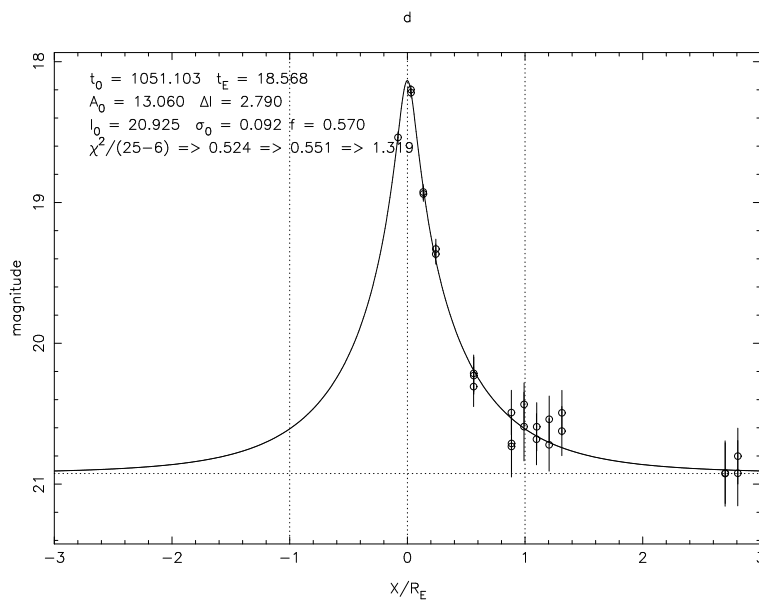


Figure 4. Fitted light-curve for the event 98BLG42. R-magnitude is plotted versus time in units of  $t_E$ . The slight increase in brightness in the region  $x/R_E \sim 1$  of the plot is probably a blending effect from a star that lies almost on top of the target. As the target becomes very faint the program has difficulty distinguishing between the two stars. The estimated event parameters are shown on the top left of the plot.

where  $\sigma_0$  is the readout noise (in ADU),  $t$  the exposure time,  $A_{psf}$  is the effective area of the point spread function,  $G$  is the gain ( $e^-/\text{ADU}$ ) and  $f_*$ ,  $f_s$  the flux from the star and flux per pixel from the sky respectively.

## 5. Results for 98BLG35 and 98BLG42

Our best sampled light-curves were those for the events MACHO 98BLG35 (fig 3) and 98BLG42 (fig 4). The observations of these events started approximately at the time of maximum amplification. Unfortunately all of the events that we followed during the observing period were sampled only in the decline, with the exception of 98BLG42 where we had one point before maximum amplification. For this reason our fits to the data, although in agreement with the fits by other groups, do not yield useful constraints on the event parameters.

Figure 5 shows the accuracy achieved for 390 stars on all the frames and the theoretical error curves. Due to poorer seeing and brighter sky at airmass 1.5-2, the dominant source of noise in our data was sky noise. Photon noise from the star is important only for stars brighter than 15th magnitude. The measured RMS scatter of repeat measurements is generally close to theoretical estimates. However, some of the data points scattered by more than the expected value. These stars were identified later in the frames and were seen to be suffering from overcrowding.

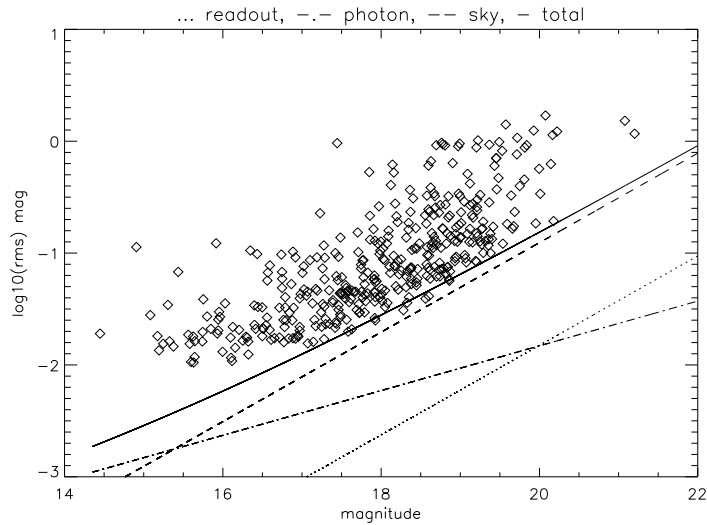


Figure 5. R-magnitude values versus the corresponding rms values for 390 stars. The plot looks noisier than expected which is due to the overcrowding of some stars.

## 6. Significance of the results

We have achieved photometric measurement errors with a lowest value of  $\sim 1\text{-}2\%$ . This is also comparable to the photometric accuracy reported by other microlensing teams that operate at low airmass from the advantageous (for Galactic Bulge observations) environment of southern observatories. We believe that our results show that microlensing observations in the Galactic Bulge looking for Jupiters can also be successfully performed from northern sites and with small telescopes.

## References

- Paczynski B. 1996 in ARA&A, 34, 419  
 Bennet D. & Rhie S. 1996 in ApJ, 472, 660  
 Gould A. & Loeb A. 1992 in ApJ, 396, 104  
 Penny A. 1995 Starlink Documentation